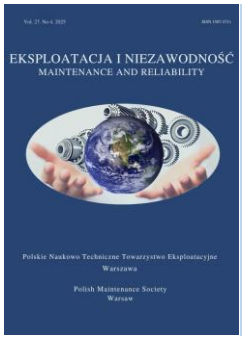

Eksploatacja i Niezawodnosc – Maintenance and Reliability

Volume 27 (2025), Issue 4

journal homepage: http://www.ein.org.pl

Article citation info:
Cheng L, Gao H, Sun W, Chen C, Xu X, An Integrated Method for Predictive State Assessment and Path Planning for Inspection Robots in Island-Based Unmanned Substations, Eksploatacja i Niezawodnosc – Maintenance and Reliability 2025: 27(4) http://doi.org/10.17531/ein/203994

An Integrated Method for Predictive State Assessment and Path Planning for Inspection Robots in Island-Based Unmanned Substations

Indexed by: Web of Science Group

Li Cheng[a,b], Haibo Gao[a], Wanfeng Sun[a], Can Chen[a], Xing Xu[c,*]

[a] School of Naval Architecture, Ocean and Energy Power Engineering, Wuhan university of technology, China
[b] Key Laboratory of High Performance Ship Technology, Wuhan University of Technology, China
[c] School of Electrical Engineering, Naval University of Engineering, China

Highlights

- A novel Conv2D-PSE-iTransformer improves multivariate time series predictions.
- Dynamic AHP adjusts temperature weights for transformer health assessment.
- DRL-based path planning prioritizes high-risk equipment with optimized routes.
- Simulated Annealing and Pruning enhance DRL efficiency and solution accuracy.

Abstract

To address the challenge of robotic inspection and maintenance in unmanned environments, this paper presents an integrated approach combining Conv2D-PSE-iTransformer for equipment state prediction, Dynamic Analytic Hierarchy Process (D-AHP) for health assessment, and deep reinforcement learning for optimized path planning. The Conv2D-PSE-iTransformer accurately predicts the operational state of electrical equipment, which serves as a critical input for the D-AHP evaluation. Based on the predicted state, D-AHP dynamically assesses the health of the equipment, enabling the identification of high-risk components that require immediate attention. Based on these evaluations, the DRL-based path planning generates optimized inspection routes that prioritize these high-risk areas while ensuring complete coverage with minimal inspection time. Experimental results demonstrate the effectiveness of this integrated method, highlighting its ability to reduce inspection time and enhance the overall efficiency, safety, and reliability of robotic inspections in complex, high-risk environments.

Keywords
robotic inspection**;** predictive maintenance, Conv2D-PSE-iTransformer, dynamic analytic hierarchy process, deep reinforcement learning

This is an open access article under the CC BY license (https://creativecommons.org/licenses/by/4.0/)

1. Introduction

The electrical inspection of equipment in unmanned substations on remote islands is critical for ensuring the safe operation of equipment and maintaining system stability[1-3]. These facilities are often exposed to harsh environmental conditions, such as high temperatures, salt spray, and hurricane, which accelerate equipment aging and increase the risk of failures [4-6]. Consequently, timely and accurate electrical inspections are essential to guarantee the reliability and integrity of island-based power systems [7].

Traditional manual inspection methods are severely limited in such isolated and hazardous environments, suffering from low efficiency and posing significant safety risks to personnel. As a result, intelligent electrical inspection robots equipped with high-precision, multi-parameter real-time monitoring

(*) Corresponding autho
E-mail addresses: L. Cheng (ORCID: 0009-0008-5883-3810) chengli@whut.edu.cn, H. Gao (ORCID: 0000-0002-9349-9722) hbgao_whut@126.com, W. Sun (ORCID: 0009-0003-4828-6642) swf01326@whut.edu.cn, C. Chen (ORCID: 0009-0007-8514-1273) C_Chen@whut.edu.cn, X. Xu (ORCID: 0009-0004-2086-7610) xuxin19901201@126.com

capabilities have become indispensable[8, 9]. These robots can perform routine inspections without human intervention, effectively mitigating safety risks in complex conditions [10].

The intelligent electrical inspection robot system collects temperature and vibration data from electrical equipment to perform predictive analysis and comprehensive health assessments. This enables early fault detection and diagnosis [11, 12], significantly enhancing the scientific basis for maintenance decision-making. As a result, unplanned downtime is effectively reduced [13], ensuring the stable and efficient operation of island-based substations [14]. The deployment of intelligent inspection robots in unmanned substations on remote islands not only enhances inspection safety and coverage [15] but also significantly boosts equipment reliability and operational cost-efficiency[4, 16]. However, the intricate layout of electrical equipment introduces considerable challenges for inspection path planning, which is often subject to high levels of uncertainty and dynamic changes[17, 18]. Therefore, intelligent inspection systems must be equipped with robust adaptive capabilities to ensure the effective and efficient execution of inspection tasks.

1.1. Literature review

Predictive maintenance of equipment is a critical technology for ensuring the reliable operation of power systems. Current approaches to predictive maintenance predominantly leverage time series analysis [19, 20] and machine learning [21, 22], including methods such as Support Vector Machines (SVM) [23, 24], Long Short-Term Memory (LSTM) networks[25], and physics-based predictive models [26, 27]. These methods utilize historical data to construct models capable of predicting equipment health to support maintenance decision-making. Bakdi et al.[28] proposed a weakly supervised machine learning approach based on Multi-Instance Learning and Random Forests (RF) to analyze event logs from propulsion systems, enabling intelligent predictive maintenance. Similarly, Cipollini et al. [29] introduced a data-driven model that combines sensor historical data from propulsion systems with supervised data analysis techniques to implement precise, condition-based maintenance. This approach facilitates monitoring of equipment health and prediction of maintenance needs. However, traditional state prediction methods often struggle to address the challenges posed by highly dynamic and complex operational environments[30]. In island-based substations, where diverse types of equipment operate under harsh conditions with high interdependencies, these limitations become even more pronounced. Therefore, more adaptive and robust predictive methods are required to evaluate equipment operating conditions accurately, thereby enhancing the overall system reliability.

The Analytic Hierarchy Process (AHP) is widely regarded as an ideal tool for assessing the condition of power equipment due to its strengths in multi-criteria decision-making, flexibility in priority setting, capacity to handle uncertainty and subjective judgments, strong compatibility, high transparency in evaluations, and optimization of resources [31]. Panmala et al. [32] developed a methodology that translates visible aging into numerical scores while incorporating condition factors to account for invisible aging and environmental influences, facilitating the comprehensive evaluation of gas-insulated switchgear. Similarly, Tanaka et al. [33] introduced a multi-criteria evaluation framework based on AHP and pairwise comparisons to assess the health of substation equipment. This approach integrates multiple indicators to determine health levels and prioritize maintenance and upgrade planning. Hernandez et al. [34] further leveraged AHP to rank critical criteria for power equipment and employed pairwise comparisons to identify the most appropriate condition monitoring systems. Despite its extensive adoption across various domains, the traditional AHP framework is inherently static and struggles to accommodate dynamic and evolving decision-making scenarios [35].

The traditional AHP framework is unable to capture changes in equipment condition over time, leading to a lack of flexibility in long-term assessments and making it challenging to accommodate dynamic adjustments to equipment states [36]. To address this limitation, Raharjo et al.[37] proposed a time-dependent compositional data forecasting approach. This method tackles the problem of changing AHP priorities over time by applying exponential smoothing, enabling dynamic priority prediction even when historical data is limited. The Dynamic AHP (D-AHP) framework offers significant advantages in responding to environmental changes and fluctuating decision-making conditions over time [30, 32]. By

dynamically adjusting priority weights based on temporal or contextual variations, D-AHP facilitates adaptive scheduling of maintenance tasks, reduces overall maintenance costs, and ensures high equipment availability[14].

Inspection robots leverage comprehensive analyses of equipment health conditions to prioritize high-risk areas, avoid obstacles, and optimize their inspection paths. This approach ensures complete coverage while minimizing inspection time, enabling efficient task execution and enhancing operational performance [38]. Traditional path planning algorithms, such as A*(A-Star), Rapidly-Exploring Random Tree (RRT), and Dijkstra, are widely used for determining optimal inspection routes [39]. Zhao et al. [40] developed a hybrid navigation algorithm that integrates reflectors and lasers with a dynamically weighted RRT algorithm, enabling cooperative path planning among multiple robots. Similarly, Azpúrua et al. [41] employed the Dijkstra algorithm to calculate optimal paths by minimizing costs related to distance, energy consumption, or terrain complexity, facilitating the safe and efficient traversal of challenging terrains. In another study, Khanam et al. [42] introduced a priority-enabled coverage path planning approach designed for autonomous inspections across multiple disconnected regions, particularly in hazardous or inaccessible areas. While these methods are effective in deterministic environments, they face significant limitations when dealing with the medium- to high-risk, dynamic, and uncertain conditions often found in electrical substation settings. Such environments demand more adaptive and resilient path planning strategies to address the inherent complexity and variability.

In recent years, reinforcement learning-based path planning methods have gained significant traction in inspection tasks, especially within complex and high-risk environments. Among these, Q-learning is one of the most prevalent algorithms, renowned for its ability to optimize path planning by learning optimal policies, thereby improving both the efficiency and safety of inspection operations [43]. Low et al. [44] enhanced the initialization of Q-values by integrating global and local searches within the Flower Pollination Algorithm framework. This innovation endowed robots with preliminary environmental knowledge during the early stages of path exploration, resulting in accelerated convergence. Similarly, Yu et al. [45] introduced the Double Deep Q-Network algorithm, which formulates adaptive obstacle avoidance strategies for dynamic scenarios through reinforcement learning. Their model, grounded in state and reward functions, significantly improved the autonomous navigation capabilities of agricultural robots in complex farmland environments. Barros et al. [46] proposed an adaptive approach combining Reinforcement Learning (RL) and Learning Automata. By employing offline learning in simulated environments alongside heuristic search techniques, their method enabled effective path-following control and robust planning.

Deep Reinforcement Learning (DRL) algorithms build on traditional reinforcement learning by incorporating neural networks, enabling dynamic optimization of path planning in real-world environments. This approach not only enhances the adaptability of reinforcement learning to unfamiliar states but also significantly improves its efficiency in addressing complex challenges [47, 48]. Hadi [49] utilized the Twin Delayed Deep Deterministic Policy Gradient algorithm to achieve real-time path planning and control for autonomous underwater vehicles operating in unknown ocean environments, effectively ensuring precise motion control and obstacle avoidance. Similarly, Krishna et al. [50] employed a hybrid architecture combining Convolutional Neural Networks (CNN) with LSTM networks, alongside the Actor-Critic Experience Replay algorithm. This approach enabled robots to execute low-cost coverage in real-time scenarios, substantially enhancing coverage efficiency by optimizing path lengths and minimizing unnecessary shape transitions. Ren et al. [51] tackled the limitations of conventional DRL algorithms, such as slow convergence and a tendency to get trapped in local optima, by introducing a data collection method based on Dynamic Programming. This method generated high-quality training data, which, when combined with Extreme Learning Machine for initializing network parameters, resulted in a two-stage DRL framework that improved learning speed and performance. Despite these advancements, existing research continues to face significant challenges in integrating equipment condition predictions and risk assessment results for effective real-time path adjustment.

1.2. Proposed approach

This study introduces a novel Complete Coverage Path Planning (CCPP) method tailored to inspection tasks in island-

based substations. The proposed approach seamlessly integrates advanced state prediction, health assessment techniques, and a DRL-based framework to achieve enhanced performance. The methodology begins with the use of the Parallel Series Embedding (PSE) framework, augmented by 2D Convolution (Conv2D) and iTransformer techniques, to accurately predict the operational conditions of electrical equipment. These predictions provide reliable inputs for downstream analyses. Subsequently, the Dynamic Analytic Hierarchy Process (D-AHP) is applied to evaluate equipment health, offering a systematic and adaptive framework for health assessment. Based on the health evaluation outcomes, a newly designed DRL algorithm is employed for CCPP of inspection robots. The algorithm dynamically adjusts inspection routes in real-time, adapting to evolving equipment conditions to optimize task efficiency. By synergizing predictive modeling, health evaluation, and DRL-based path planning, the proposed method achieves significant improvements in inspection accuracy and responsiveness. It reduces both time and energy consumption, ultimately enhancing the operational and maintenance efficiency of island-based power systems.

2. Timing prediction of electrical equipment

Whether dispatched to inspect a malfunctioning system or deployed to perform on-site maintenance tasks, robotic inspection and maintenance operations can incur significant time delays, particularly when responding to unexpected equipment failures. These time demands can lead to inefficiencies and prolonged system downtime. To address this issue, predictive maintenance plays a crucial role. By proactively scheduling inspection and maintenance tasks, it helps reduce unnecessary delays, thereby enhancing overall operational efficiency and system reliability.

Transformers are critical components in substation power systems, where their reliable operation directly impacts the stability and efficiency of electricity distribution. Predicting transformer oil temperature is paramount for monitoring the operational status and assessing the health condition of transformers. Accurate predictions can effectively provide early warnings of potential failures, extend the lifespan of the equipment, and enhance the reliability of the power grid. However, multivariate time series data often pose challenges, such as feature complexity, long-short term dependencies, and missing features for future time steps [52]. Traditional models struggle to capture nonlinear dynamics and complex dependencies between variables, often introducing noise or redundancy, which can compromise prediction accuracy. To address these challenges, we propose a novel structural framework, Conv2D-PSE-iTransformer, which integrates the PSE module with Conv2D and iTransformer. The Conv2D-PSE module processes temperature features, while iTransformer handles contextual features, preserving their individual properties. The convolutional layers extract local temporal patterns, thereby enhancing the performance of multivariate modeling [53].

2.1. The Conv2D-based Parallel Series Embedding Module

Convolutional Neural Networks (CNNs) have become widely adopted for extracting features from time series data, with 2D Convolution (Conv2D) [54] standing out for its ability to capture local patterns and interdependencies across multiple variables. Time series data is typically represented as a two-dimensional tensor, where each row corresponds to a different feature, and each column represents a time step. Conv2D leverages convolutional filters that slide across both the temporal and feature dimensions, effectively extracting local dynamic characteristics and correlations among variables. In this study, Conv2D is utilized within the Parallel Series Embedding (PSE) [55] module, which aims to efficiently embed both the target sequence and contextual features.

Time series data is typically represented as a 2D tensor $X \in R^{T\times F}$, where T denotes the number of time steps and F represents the feature dimension. The Conv2D operation extracts the local dynamic features of the time series and the correlation between features by sliding the convolution kernel in the time dimension and feature dimension. The specific computation is given by the following formula:

$$Y(i,j) = \sigma\left(\sum_{m=1}^{H}\sum_{n=1}^{W} X(i+m, j+n)\cdot\theta(m,n) + b\right) \quad (1)$$

Where, $\theta \in R^{H\times W}$ is the convolutional kernel, H and W are the kernel sizes along the temporal and feature dimensions, respectively, b denotes the bias term, and σ is the activation function; $Y \in R^{(T-H+1)\times(F-W+1)}$ is the input feature map, capturing the local patterns of the tensor.

In the proposed framework, the target sequence and contextual features are processed independently using separate Conv2D layers, ensuring that the trend information of the target values and the inter-variable dependencies of contextual features are modeled separately. The Conv2D layers utilize a kernel size of $H = 1$ to capture short-term dynamic patterns along the temporal dimension, while $W = 1$ is applied to model individual feature variables. Furthermore, causal parameters [54] are applied to constrain the receptive field of the convolutional kernel, ensuring that it covers only the current and preceding time steps. This prevents the incorporation of future information and enhancing the model's interpretability and adaptability.

2.2. iTransformer

The iTransformer [56] is an innovative Transformer architecture specifically designed for time series forecasting tasks, enhancing the modeling of time series and multivariate features through a deliberate inversion of the core functions within key modules. Unlike traditional approaches, which treat time steps as the fundamental units (time-step tokens), the iTransformer utilizes the variables themselves as the central modeling units (variable tokens). The architecture comprises an encoder, with an optional decoder, and is constructed to capture both the intricate interdependencies among variables and the global temporal patterns. This design enables the iTransformer to handle multivariate time series tasks more effectively by inherently modeling variable interactions while simultaneously reducing computational complexity, thus improving both modeling efficiency and interpretability.

Like the core Attention Mechanism in the standard Transformer [57], the iTransformer also utilizes Multi-Head Attention to model the relationships between variables. The input variable tokens are projected linearly to produce the Query (Q), Key (K), and Value (V) matrices, which are subsequently used to compute the attention according to the following formula:

$$Attention(Q,K,V) = softmax(\frac{QK^T}{\sqrt{d_k}})V$$
$$Q = HW_Q, K = HW_K, V = HW_V \quad (2)$$

Where, W_Q,$W_K$and$W_V$represent the projection matrices for the Q, K, and V vectors, respectively; H denotes the matrix of embedded variable tokens; and $d_k$indicates the dimensionality of the key vectors, which is used to scale the dot-product results.

The design of iTransformer departs from the conventional use of positional embeddings, instead utilizing a feedforward network (FFN) to implicitly capture the global patterns in time series data. This innovative architecture further improves the model's predictive accuracy and generalization ability. By employing this reversed structure, iTransformer provides a robust solution for multivariate time series forecasting, particularly excelling in scenarios characterized by complex inter-variable dependencies.

2.3. Conv2D-PSE-iTransformer

This study presents the Conv2D-PSE-iTransformer architecture, which integrates an enhanced PSE Module with the iTransformer structure, providing an effective solution for multivariate time series forecasting tasks. Using the PSE Module, target values and contextual features are independently processed via Conv2D, facilitating the extraction of local dynamic patterns along the time dimension and identifying dependencies between contextual features. The key implementation of this module is demonstrated in the pseudocode in Table 1, which highlights the application of causal masking to prevent future information leakage, as well as the reduction of feature dimensionality to alleviate computational complexity. The resulting Q_f, K_f, and V_f vectors are input into the iTransformer, providing an efficient feature representation for subsequent global modeling.

In the iTransformer, the variable H is utilized to model the dependencies between various feature variables. The Multi-Head Attention mechanism enables the calculation of feature interactions across multiple subspaces, while the FFN further captures global patterns along the temporal dimension, allowing the model to simultaneously capture short-term trends and long-term dependencies. Ultimately, predictions for future time steps are generated through linear projection. The overall methodology is comprehensively presented through pseudocode, which illustrates the logical flow from parallel embedding to iTransformer modeling. Its modular design ensures both efficiency and adaptability, making it especially suitable for complex multivariate time series tasks.

Table 1: Pseudo code for Conv2D-PSE-iTransformer

Input: $\boldsymbol{X_{target} \in R^{T\times 1}}$:Target value time series, length T;
$\boldsymbol{X_{context} \in R^{T\times F}}$: Context features time series, F is the number of features.

Output: $\boldsymbol{Y_{perd} \in R^{\tau\times 1}}$: Predicted future time steps, length $\boldsymbol{\tau}$

Parameters: d_model :Embedding feature dimension; $kernel\_size$: Convolution kernel size for local feature extraction; num_heads: Number of attention heads; num_layers: Number of layers in iTransformer

Prat 1 Parallel Series Embedding Module
Function PSE (X_{target}, $X_{context}$, $\boldsymbol{d\_model}$, $\boldsymbol{kernel\_size}$)
Step1: Target value Embedding
$Y_{target} = Conv2D(X_{target}, kernel\_size = (1, kernel\_size))$
$Q_z, K_z, V_z = LinerProjection(Y_{target}, d\_model)$
Step2: Contextual feature Embedding
$\boldsymbol{Y_{context} = Conv2D(X_{target}, kernel\_size = (1, kernel\_size))}$
$Y'_{context} = ApplyCasualMask(Y_{context})$ # Ensuring time consistency
$Y''_{context} = CompressFeatureDimension(Y'_{context}, target\_dim = 1)$
$Q_f, K_f, V_f = LinerProjection(Y''_{context}, d\_model)$
Return $Q_z, K_z, V_z, Q_f, K_f, V_f$

Part 2 iTransformer Module
Function iTransformer $(Q_z, K_z, V_z, Q_f, K_f, V_f, num\_heads, num\_layers)$
Step1: $H = InitializeTokens(Q_z, K_z, V_z, Q_f, K_f, V_f)$
Step2: Multi-layer Transformer structure
for layer in range (num_layers):
$Attention\_H = MultiHeadAttention(H\_init, num\_heads)$
$H = FeedForwardNetwork(Attention\_H)$
Step3: Final Projection
$Y_{pred} = ProjectionLayer(H\_updated)$
Return Y_{pred}

Part 3 Main
Function main (X_{target}, $X_{context}$)
$Q_z, K_z, V_z, Q_f, K_f, V_f = PSE(X_{target}, X_{context}, d\_model = 128, kernel\_size = 3)$
$Y_{pred} = iTransformer(Q_z, K_z, V_z, Q_f, K_f, V_f, num\_heads = 8, num\_layers = 6)$
Return Y_{pred}

Where, Y_{target} is the target sequence after Conv2D processing, Q_z, K_z, V_z is Query, Key, and Value vectors for the target sequence, $Y_{context}$ is the context feature sequence after the initial Conv2D operation, representing extracted temporal patterns; $Y'_{context}$ is the result after applying the causal mask to ensure temporal consistency; $Y''_{context}$ is the Feature dimension compressed representation of context features; Q_f, K_f, V_f is Query, Key, and Value vectors for context features.H represents the combined embeddings of target and context features, used as input for iTransformer; $Attention\_H$ is the output of the Multi-Head Attention mechanism at each layer, capturing dependencies between variables.

3. Dynamic health status assessment of unmanned power stations

Predictive maintenance, a key application of condition-based assessment, enables the identification of potential faults through continuous monitoring and analysis of equipment performance data, thereby facilitating proactive interventions [34]. In contrast to traditional fixed-schedule maintenance, this approach is not only more cost-effective but also substantially reduces unnecessary downtime and maintenance costs.

This study uses the health condition of transformers as a case study to evaluate the status of critical electrical equipment in substations. The Dynamic Analytic Hierarchy Process (D-AHP) offers a robust and adaptive framework for condition assessment. By dynamically integrating multiple evaluation criteria and considering the evolving nature of operational and environmental conditions, this method enhances real-time adaptability, thereby improving both the accuracy and relevance of the assessment.

3.1. Health Assessment of Transformers Using AHP

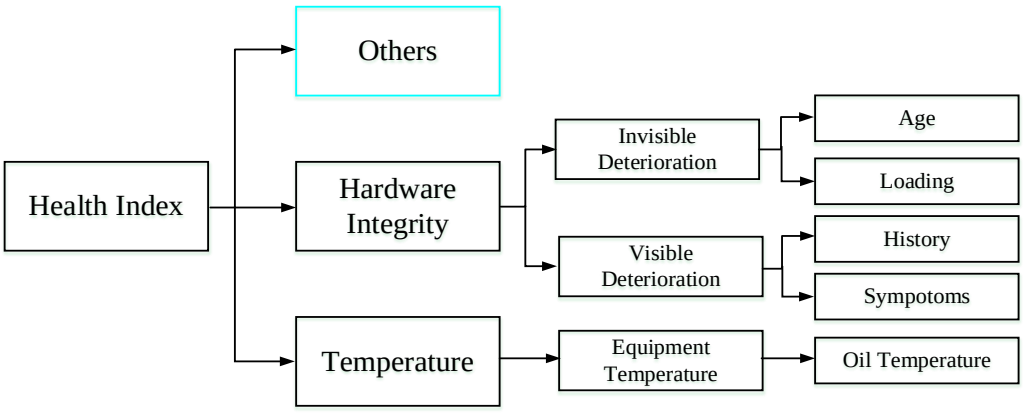

Figure 1. Transformer equipment health and standards.

To assess the health status of transformer equipment, a comprehensive set of evaluation criteria tailored to substation transformers has been developed, based on expert knowledge [58, 59]. These criteria encompass parameters such as oil temperature, gas content, load, electrical test parameters, equipment age, maintenance history, fault symptoms, climate and environmental conditions, and oil quality. Among them, oil temperature, equipment age, load, maintenance history and fault symptoms can effectively reflect the operating status of the transformer and have high practical operability. To simplify the model and enhance assessment efficiency, this study primarily focuses on these five critical parameters, as shown in Figure 1.

3.2. Health assessment of transformers using D-AHP

Although the traditional AHP method is widely adopted across various domains, its static nature renders it ill-suited for dynamic decision-making scenarios where conditions continuously evolve. Dynamic AHP (D-AHP) addresses this limitation by incorporating temporal dependencies, decomposing the decision problem into more tractable subproblems, and dynamically adjusting priorities in response to shifting conditions, thereby ensuring adaptability to changing environments [35, 60]. For instance, when a transformer's oil temperature significantly deviates from its normal range, a static AHP approach would retain the same weight for the temperature criterion as it would under normal operating conditions. This static method fails to account for the real-time influence of critical parameters on the overall health index, which may lead to the delayed identification of emerging risks or abnormal behaviors.

To address this issue, we propose an enhanced framework that dynamically adjusts the weight of the temperature criterion according to the observed operating conditions. Specifically, the weight assigned to oil temperature is dynamically modified according to the degree of deviation from the normal range, ensuring that the health index accurately reflects the transformer's real-time status. This dynamic adjustment process utilizes the D-AHP, which integrates the traditional AHP with dynamic weight allocation. This approach not only enhances the accuracy of health assessments but also provides a more reliable foundation for decision making under varying operational conditions. The weight calculation method is presented in Fig 2.

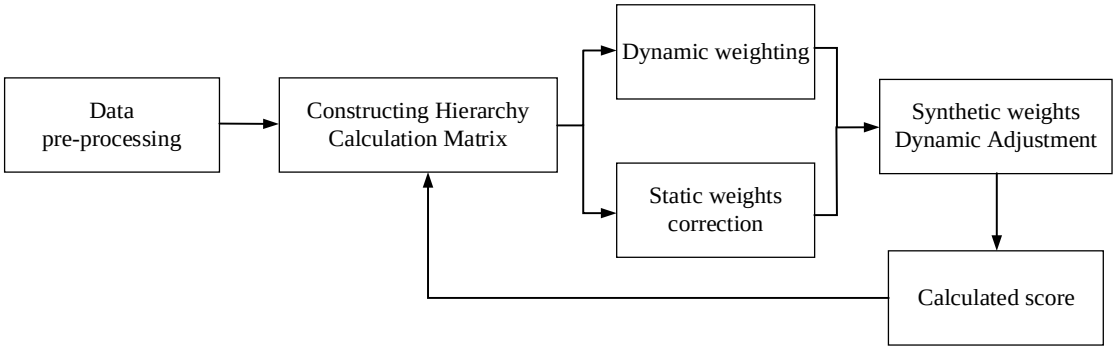

Figure 2. Process of calculating dynamic weights for health assessment using D-AHP.

This framework integrates oil temperature prediction data with other static criteria into a hierarchical calculation matrix, facilitating the dynamic evaluation of transformer health. Initially, the oil temperature data is preprocessed to eliminate noise and inconsistencies, thus laying the foundation for dynamic weighting. This preprocessing step ensures the reliability of the data and provides accurate inputs for subsequent health assessments. Based on the deviation of the oil temperature from normal operating conditions, the framework assigns varying weights to the temperature, thereby enabling real-time responses to temperature anomalies. The weight update formula is as follows:

$$\omega_i(t) = \frac{\sum_{j=1}^{n} a_{ij}(t)}{\sum_{i=1}^{n}\sum_{j=1}^{n} a_{ij}(t)} \tag{3}$$

Where, $\omega_i(t)$ represents the weight of criterion C_i at time t, $a_{ij}(t)$ denotes the matrix judgment element derived from the comparison between criteria C_i and C_j at time t, and n refers to the total number of evaluation criteria. Through dynamic adjustment, the weight of oil temperature can fluctuate in response to changes in the operational status of the equipment, thereby ensuring the system's real-time responsiveness to anomalies. Additionally, the weighting of static criteria (e.g., age, load, support history, and symptoms) are also adjusted at each assessment to preserve the overall balance and accuracy of

the assessment.

The dynamically updated and corrected weights are aggregated to generate a comprehensive health score, which accurately reflects the current condition of the transformer. This score is then fed back into the system's hierarchical computation matrix, facilitating iterative adjustments that enhance adaptability to changing conditions. By incorporating dynamic adjustments and feedback, the framework enhances the accuracy and reliability of health assessments, thereby facilitating proactive maintenance and informed decision-making.

3.3. From health assessment to actionable maintenance mapping

As shown in Figure 3, the Conv2D-PSE-iTransformer framework proposed in this study effectively forecasts key performance indicators essential for transformer health, with particular emphasis on oil temperature. By incorporating the Dynamic Analytic Hierarchy Process (D-AHP), the framework dynamically adjusts the weight assigned to the temperature criterion, thereby ensuring that health assessments are adaptable to real-time conditions. This method preserves the relative stability of static weights for factors such as equipment age and maintenance history, while providing a comprehensive and responsive evaluation framework. Consequently, it successfully integrates prediction, assessment, and decision-making processes, thereby offering valuable support for proactive maintenance strategies.

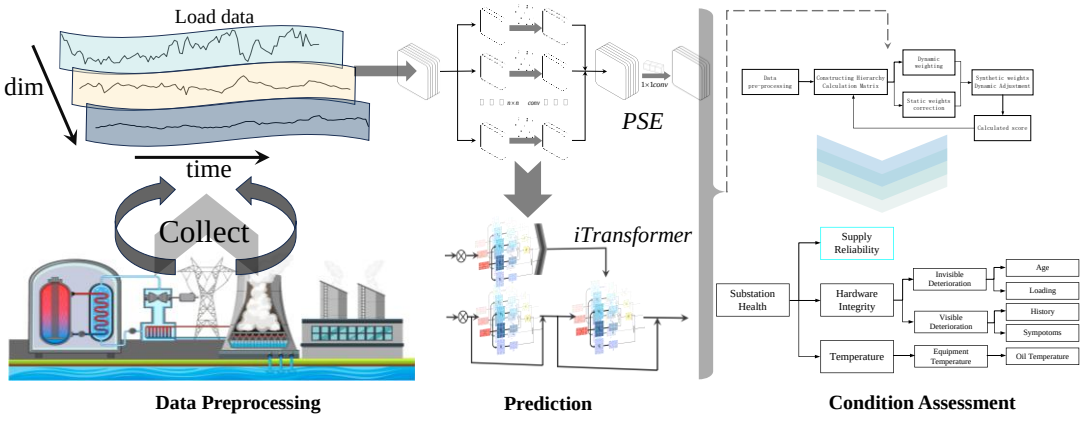

Figure 3. Predictive maintenance framework for transformer state estimation and evaluation.

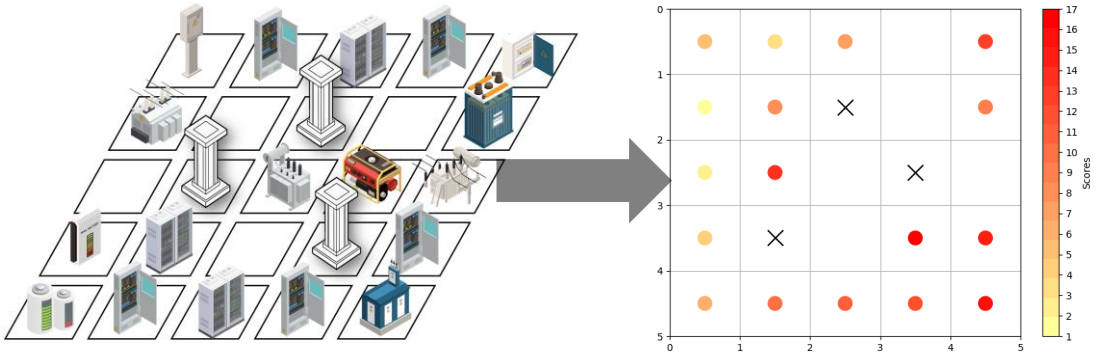

Figure 4. Transformation to simplified 2D map for maintenance planning.

Subsequently, the aforementioned methodology was applied to assess the health status of 17 critical electrical components at an island substation in the East China Sea, employing a variety of assessment criteria. Based on the calculated health scores, the components were ranked to prioritize maintenance and inspection activities. To enhance visualization and operational efficiency, components with varying health scores were assigned distinct color codes, enabling rapid identification of their respective statuses. Furthermore, the evaluation results were incorporated into a simplified map, thereby streamlining subsequent inspection and maintenance tasks, as shown in Figure 4. It is important to note that, in this experiment, the model was simplified by excluding factors such as equipment size, with the primary focus placed on optimizing the substation

layout and inspection pathways at the island substation.

4. Deep Reinforcement Learning for complete coverage path planning

Due to the critical importance of island substations, regular and efficient inspections are essential for ensuring their operational safety and reliability. Predictive maintenance plays a pivotal role in enhancing inspection efficiency by enabling timely assessments of the health status of electrical equipment. Based on the health status maps generated through equipment evaluations, this study proposes a path planning method that leverages Deep Reinforcement Learning (DRL) for comprehensive substation inspection. The approach integrates Attention Mechanisms with Reinforcement Learning (RL) algorithms: a policy network guides the selection of node pairs, while a value network evaluates the actions taken, enabling iterative refinement of the solution. Additionally, to optimize path planning and enhance algorithmic efficiency, simulated annealing and pruning algorithms are incorporated. These techniques streamline the path selection process by eliminating redundant nodes and dynamically adjusting the route, thereby improving the overall optimization performance of the inspection path. By combining the feature extraction capabilities of Deep Learning (DL) with the optimization and exploration strengths of reinforcement learning, the proposed method effectively addresses complex path planning challenges, demonstrating robust generalization across diverse operational scenarios.

4.1. Deep Learning based on Transformer

In the DRL framework proposed in this study, the DL components are pivotal in capturing the intricate interdependencies between nodes and in generating and evaluating high-quality strategies for path optimization. The architecture primarily integrates a policy network and a value network, both of which leverage the robust capabilities of deep neural networks to achieve the RL objectives of path optimization.

The policy network within this framework is constructed upon a deep neural architecture, as shown in Figure 5. It incorporates Multi-Head Attention Mechanisms, fully connected layers, and normalization layers to model both global and local relationships among nodes. Initially, node features, including their coordinates and scores, are projected into a high-dimensional space through a linear projection layer. These embeddings are subsequently processed by stacked self-attention layers, which, in conjunction with residual connections and batch normalization, capture long-range dependencies among nodes. The output of the attention layers is further refined through fully connected layers to model complex nonlinear relationships and is subsequently aggregated through global max pooling to extract key features.

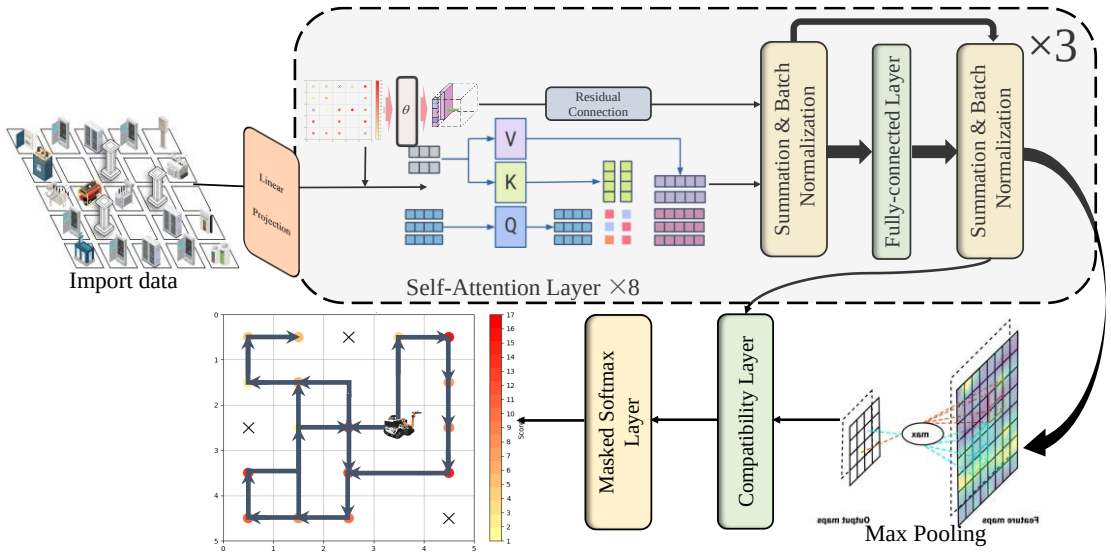

Figure 5. Transformer-based Policy Network.

The final layer of the policy network comprises a compatibility layer and a masked max layer, which serve to map the extracted features to a probability distribution of potential actions, such as node pair swaps. Actions are sampled

from the generated probabilities, enabling the agent to select actions that interact with the environment by modifying the solution state. The network is trained within a reinforcement learning framework, where the policy gradient is updated based on the rewards received from the environment, ensuring that the policy progressively converges to generate more optimized solutions over time. The resulting embeddings are utilized to generate a probability distribution $\pi = (a|s;\theta)$ over potential actions, with θ representing the parameters of the policy network, which directly guide the agent's decision-making process and enable continuous improvement of the proposed path. The optimization of the policy network aligns with the reinforcement learning objective of maximizing the expected cumulative reward:

$$J(\theta) = E_{\pi_\theta}[\sum_{k=0}^{K} R_k] \quad (4)$$

Where, R_k is the reward at time step k, and E_{π_θ} denotes the expectation over all possible paths of the policy π_θ. This approach, which integrates the attention mechanism with reinforcement learning, allows the network to effectively explore and exploit the solution space.

In this framework, the value network, commonly referred to as the critic network， is responsible for estimating the value of a given state within the solution space during the optimization process. In contrast to the policy network, which is primarily responsible for generating action probabilities, the value network predicts a scalar value representing the expected cumulative reward for a given state[61]. In the current implementation, the value network employs a feedforward architecture with fully connected layers to process and encode the environmental input features. The node features (e.g., coordinates and scores) are initially embedded into a high-dimensional space. These embeddings are then passed through a series of fully connected layers with nonlinear activation functions, each capturing increasingly abstract representations of the solution state. To stabilize the training process and enhance convergence rates, batch normalization is applied to intermediate outputs. The resulting value estimates inform the policy network, allowing it to adjust the policy in favor of higher-value states, thereby driving the optimization process. The value network plays a pivotal role in evaluating the effectiveness of the agent's actions and is integral to the continuous refinement of the policy, thereby contributing to the overall improvement of the system's performance.

The primary advantage of this DL approach is its ability to simultaneously optimize both the policy and the value function through end-to-end learning. This architecture leverages the self-attention mechanism, enabling the model to capture long-range dependencies between nodes in the graph, thereby overcoming the limitations of traditional path planning methods that depend on manually crafted features. Additionally, by integrating deep reinforcement learning with feature embedding, the network is more capable of exploring the solution space and adapting to varying problem scales and complexities.

4.2 Actor-Critic Reinforcement Learning with path optimization

DRL method plays a central role in the proposed framework of this paper, as shown in Fig. 6, which is designed to integrate the policy network and the value network to enable efficient path optimization in dynamic environments. The DRL process begins with state perception, constructing a closed-loop system that facilitates dynamic interaction from state perception to path optimization. The state information (S_t), generated by the environment, includes the current node's position on the map, the distribution of target nodes, and historical path records. This information is passed as input to the policy network. The policy network, utilizing attention-based encoding, predicts the action probabilities corresponding to potential modifications in the current path sequence, while the value network assesses the expected rewards of these actions, effectively serving as a baseline in the training process. The value network assesses the actions chosen by the policy network by estimating the cumulative return $V_{(S_t)}$ and the advantage function $A_{(S_t,a)}$, offering feedback to the policy network. This actor-critic architecture [50] integrates policy optimization with value-based evaluation, effectively reducing the variance of policy updates via the value network, while steering the gradient direction of the policy network through the advantage function. During the reinforcement learning process, the reward signal and the discounted value of future states $\gamma \times V_{(S_{t+1})}$ collectively contribute to policy optimization. The advantage function is defined as:

$$A_{(S_t,a_{t+1})} = Reward + \gamma \times V_{(S_{t+1})} - V_{(S_t)} \quad (5)$$

Through this function, the policy network iteratively adjusts its predictions during backpropagation, progressively refining

its action selection to converge towards the optimal solution.

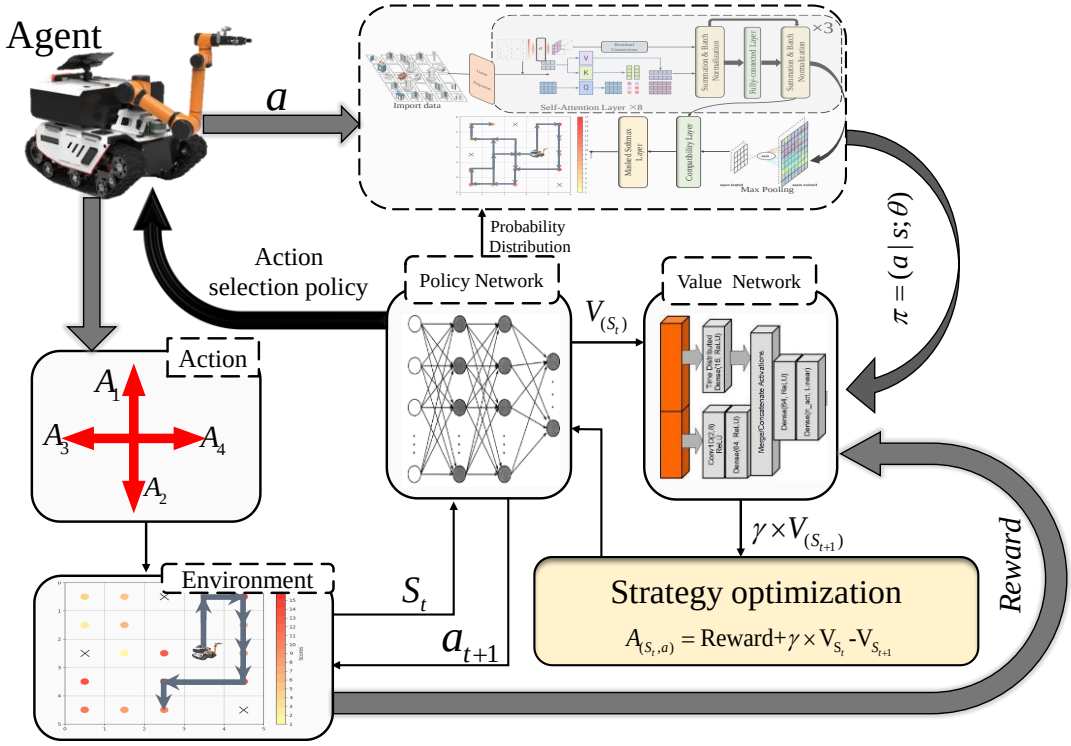

Figure 6. DRL Framework for Transformer-based Path Planning

To further refine the solution space, the RL framework incorporates Simulated Annealing and Pruning techniques. Simulated Annealing, through its progressively decreasing temperature strategy, strikes a balance between global search and local exploration, facilitating a more comprehensive exploration of the solution space in complex path planning scenarios. Meanwhile, the Pruning mechanism discards low-reward or irrelevant solutions during the optimization process, significantly narrowing the search space. The synergy of these two methods enhances the robustness of the reinforcement learning framework, enabling the model to efficiently identify the global optimum in high-dimensional, dynamic environments.

5. Results and discussion

All experiments in this study were conducted on a consistent computational platform to ensure the reliability and comparability of results. The computing system is equipped with an AMD Ryzen 7 processor operating at 3200 MHz. The dataset used in this study was collected from a power station on a reef island in the East China Sea.

5.1. Prediction Analysis of Conv2D-PSE-iTransformer

In the task of predicting transformer oil temperature, we conducted experiments using data from July 2022.

Table 2. Key Parameter Settings of the Proposed and Compared Models.

Parameters	Ours	PES-informer	iTransformer	Informer	Transformer	LSTM
Input channels	1	1	\	\	\	\
Output channels	512	512	\	\	\	\
Convolution kernel size	3	3	\	\	\	\
Encoder input sequence length	60	60	60	60	60	\
Batch Size	32	32	32	32	32	32
Number of Heads	32	32	32	32	32	\
Scaling Factor	1	1	1	1	1	\

To assess the performance of the proposed Conv2D-PSE-iTransformer model in capturing oil temperature trends, we compared it with other classical models, including iTransformer, Informer, Transformer, PSE-Informer with Conv2D and LSTM.

The key parameter settings for each algorithm are summarized in Table 2. The primary objective of the experiment was to evaluate each model's ability to predict short-term fluctuations and long-term trends, particularly regarding the transformer oil temperature data from early July 2022. The experimental results, presented in Figure 7, compare the predicted curves from different models with the actual oil temperature values in the test set.

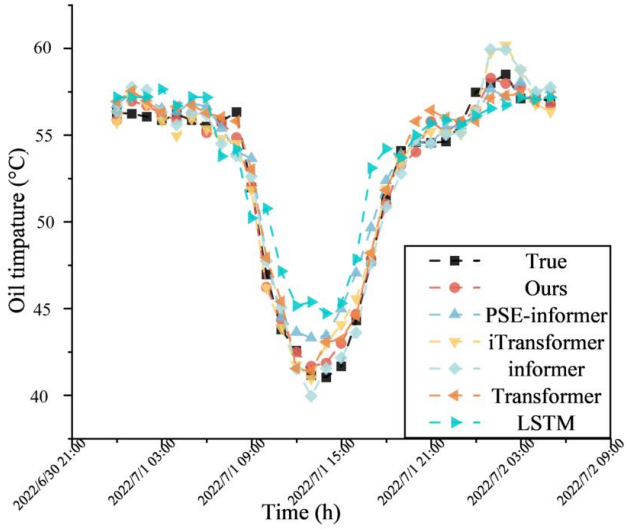

Figure7. Comparison of different methods for predicting transformer oil temperature.

As shown in Figure 7, the Conv2D-PSE-iTransformer exhibits exceptional accuracy in capturing both short-term fluctuations and long-term trends of oil temperature, with the predicted curves closely aligning with the actual values. This demonstrates that the proposed method, by integrating Conv2D into the Parallel Series Embedding (PSE) module to first extract local features of the time series, and subsequently combining it with the iTransformer module, effectively enhances the model's ability to represent short-term dynamic changes and long-term patterns.

In contrast, while the Transformer model effectively captures global dependencies, it exhibits noticeable discrepancies in both short-term and long-term predictions, leading to significant deviations from the true values. The LSTM model performs the weakest among all evaluated approaches, showing substantial prediction errors, particularly in modeling long-term trends. The iTransformer produces smoother prediction curves and captures long-term trends more effectively; however, it struggles with short-term variations, resulting in reduced accuracy for rapid fluctuations. The Informer, designed for long-range time series forecasting, shows improvements in handling extended temporal dependencies but lacks the capability to accurately model local features, leading to deviations in short-term predictions. The PSE-Informer, which incorporates Conv2D for local feature extraction, demonstrates enhanced short-term accuracy. However, its limited ability to model global dependencies prevents it from achieving the same level of long-term predictive performance as the proposed Conv2D-PSE-iTransformer model.

These findings suggest that the Conv2D-PSE-iTransformer provides a more comprehensive and balanced representation of both short-term and long-term patterns, offering improved predictive accuracy compared to the baseline models.

To further quantify the predictive performance of each model, we calculated the Mean Absolute Error (MAE) and Mean Squared Error (MSE) on the test set, as shown in Table 3. Consistent with the comparison of the prediction curves, the Conv2D-PSE-iTransformer achieves significantly lower MAE and MSE values than the other baseline models.

Table 3. Comparison of loss values in oil temperature prediction by different methods.

Methods	Ours	PSE-informer	iTransformer	informer	Transformer	LSTM
MAE	1.322059	1.458531	1.628284	1.657975	1.709213	1.941401
MSE	5.980411	7.202597	8.511854	8.951056	9.847434	11.1570501

Table 3 presents a quantitative comparison of model performance based on MAE (Mean Absolute Error) and MSE (Mean Squared Error) values. The proposed Conv2D-PSE-iTransformer achieves the lowest prediction errors, with an MAE of 1.322059 and an MSE of 5.980411, demonstrating its superior accuracy and robustness in transformer oil temperature prediction. In contrast, the baseline models exhibit significantly higher errors: the PSE-Informer achieves an MAE of 1.458531 and an MSE of 7.202597, while the iTransformer and Informer show even higher errors, with MAE values of 1.628284 and 1.657975, and MSE values of 8.511854 and 8.951056, respectively. In addition, the MSE and MAE of LSTM and Transformer have the highest errors of all the compared models, reflecting their limitations in multivariate time series tasks.

While the PSE-Informer improves upon the Informer by incorporating Conv2D layers to extract local temporal patterns, it still falls short of the proposed Conv2D-PSE-iTransformer due to its limited ability to model global dependencies. These results highlight the effectiveness of the Conv2D-PSE-iTransformer in transformer oil temperature prediction, particularly its ability to balance the modeling of local features and global dependencies, leading to more accurate and robust predictions.

To evaluate the computational efficiency of the proposed Conv2D-PSE-iTransformer model, we compared its inference time with those of other baseline models, including Transformer, Informer, LSTM, Transformer, and PSE-Informer. The results are summarized in Table 4.

Table 4. Inference Time Comparison of the Proposed and Baseline Models.

Time	Ours	PES-informer	iTransformer	Informer	Transformer	LSTM
Average Time	79.07s	83.37s	63.15	68.31	84.29s	9.97s

Based on the inference time results presented in Table 4, the Conv2D-PSE-iTransformer model achieves an average inference time of 79.07 seconds, which is slightly lower than PSE-Informer (83.37s) but higher than iTransformer (63.15s) and Informer (68.31s). While the Transformer model exhibits a slightly longer inference time (84.29s), LSTM demonstrates the fastest performance, requiring only 9.97s per prediction. The slight increase in inference time for Conv2D-PSE-iTransformer can be attributed to the additional computational complexity introduced by the Conv2D layers and PSE module. However, considering that predictions are typically performed on an hourly or daily basis, this additional computational cost remains within an acceptable range and does not compromise the model's real-time applicability.

The experimental results demonstrate that the proposed Conv2D-PSE-iTransformer substantially outperforms the other comparison models in the transformer oil temperature prediction task, particularly in capturing both short-term fluctuations and long-term trends. Its innovative architecture, which integrates parallel sequence embedding with the reversed design, significantly enhances prediction accuracy. Although the model introduces additional computational steps, the increase in training and inference time is negligible in practical applications where predictions are made on an hourly or daily basis. Future research could focus on further optimizing the model's computational efficiency and expanding its application to other multivariate time series forecasting tasks.

5.2. Results of transformer health assessment using D-AHP

To evaluate the health status of substation transformers, four key parameters were identified: load, maintenance history, symptoms, and operational age. These parameters were classified into five levels of importance: equally important, moderately important, strongly important, very strongly important, and extremely important [33], as summarized in Table 5.

Table 5: Importance level of electrical equipment.

Value	Description
1	equally important
3	moderately important
5	strongly important
7	very strongly important
9	extremely important

The pairwise comparison method, grounded in the AHP, was employed to assign weights to each parameter, with evaluations performed by power system experts from the China Southern Power Grid. The resulting weights were normalized to ensure comparability. Table 6 illustrates the weight distribution of the four parameters with respect to hardware integrity for the island substation in 2022. This approach systematically incorporates expert knowledge into the evaluation framework, ensuring consistency and reliability in parameter weighting is an essential requirement for accurate equipment health assessments.

Table 6. Hardware integrity evaluation weight distribution for Jan. 2022.

Criteria	Age	Loading	History	Symptoms	Weights
Age	1	1/5	1/3	1/5	0.0735
Loading	5	1	5/3	5/7	0.3381
History	3	3/5	1	3/5	0.2206
Symptoms	5	1	5/3	1	0.3678

Based on expert recommendations, temperature is identified as a key variable in transformer health assessment due to its direct correlation with operational conditions and potential risks. In this framework, oil temperature is first analyzed as a dynamic parameter, with its weight adjusted in real time through a dedicated function to account for deviations from normal operating ranges. The results of the temperature analysis are subsequently integrated with the hardware integrity indicators to assess the health of the transformer comprehensively. This approach enables the simultaneous consideration of dynamic temperature variations and static hardware parameters, providing a systematic basis for evaluating transformer conditions.

Specifically, when the oil temperature exceeds the standard range of 40-60°C [62], its weight increases significantly to capture the elevated risk associated with abnormal thermal conditions. Conversely, under normal operating conditions, the weight of oil temperature remains relatively low, allowing greater emphasis on other static factors, such as maintenance history and operational age. This dynamic adjustment mechanism, governed by a custom-designed function, ensures that the health assessment remains responsive to environmental changes and capable of adapting to critical operational variations. The specific change formula is as follows:

$$W(T) = \begin{cases} 0.3 + 0.3 \cdot e^{-0.5 \cdot (T-30)} & T < 40 \\ 0.3 & 40 \le T \le 60 \\ 0.75 - e^{-0.1(T-60)} & T > 60 \end{cases} \quad (6)$$

To analyze the variation in parameter weights under varying operating conditions, average monthly oil temperature data sampled at the beginning of each month in 2022 were utilized to assess transformer health. The resulting weight distribution, illustrated in Figure 8, highlights the dynamic interplay between oil temperature and static parameters. During periods of elevated oil temperature, its weight increases significantly, reflecting heightened thermal risk, whereas the weights of static factors such as maintenance history and operational age are proportionally reduced. Under stable operating conditions, the weight distribution shifts to emphasize static parameters. These findings underscore the necessity of integrating both dynamic and static factors to achieve accurate and adaptive health assessments. By dynamically adjusting parameter weights, the D-AHP method enhances the accuracy of the health index, facilitating the real-time identification of high-risk equipment. This approach establishes a robust foundation for predictive maintenance, optimized resource allocation, and enhanced transformer reliability.

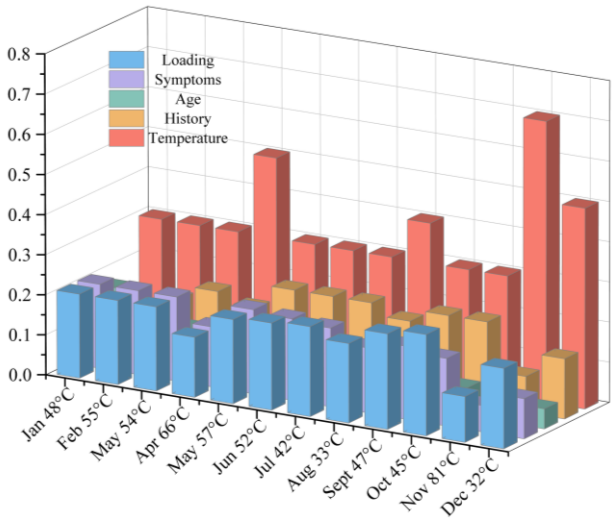

Figure 8. Weight distribution at different times and temperatures in 2022.

To further demonstrate the robustness, risk resilience, and generalization capability of the D-AHP method, we compared its health assessment results with those of the traditional AHP method and expert evaluations for different types of equipment under varying operational conditions. The comparison is summarized in Table 7.

Table 7. Comparison of Health Assessment Scores for Different Equipment.

Equipment	Parameter	Operational Condition	Expert	AHP	D-AHP
Transformer	Oil Temperature	Normal (50°C)	85	83	84
Transformer	Oil Temperature	High Risk (70°C)	60	55	62
Circuit Breaker	Operation Count	Normal (Low Operations)	88	86	87
Circuit Breaker	Operation Count	High Risk (High Operations)	58	52	60
Cable	Insulation Condition	Normal (Good Insulation)	90	88	89
Cable	Insulation Condition	High Risk (Degraded Insulation)	62	55	64

As shown in Table 7, under normal operating conditions, both D-AHP and AHP produce health assessment scores that are close to the expert evaluations, with minor deviations. However, under high-risk conditions, the traditional AHP method tends to underestimate the health score, failing to accurately reflect the increased risk. In contrast, the D-AHP method dynamically adjusts the weights of critical parameters and produces scores that are much closer to the expert evaluations, demonstrating its superior ability to capture and respond to risk factors across different types of equipment.

This comparison highlights the key advantage of D-AHP: its dynamic weight adjustment mechanism enables it to adapt to changing operational conditions and diverse equipment types, providing more accurate and reliable risk assessments. By aligning more closely with expert evaluations, especially under high-risk scenarios and across various equipment types, D-AHP has proven to be a robust and generalizable tool for health assessment in complex and dynamic environments.

5.3. Performance evaluation of DRL-based complete coverage path planning

To validate the effectiveness of the proposed improved DRL algorithm for inspecting electrical equipment at island substations, experiments were conducted using data based on equipment prioritization that were obtained through D-AHP analysis. For comparative analysis, three substations with similar configurations were included. In the experiments, priority maps for electrical equipment, derived from D-AHP analysis, were used to optimize inspection paths, as illustrated in Figure 9. Specifically, Block (a) shows the priority map for the target substation, while Blocks (b), (c), and (d) present the priority maps for the three similar substations. In the figures, regions shaded in deeper red denote higher-priority equipment, indicating components requiring more immediate inspection.

The priority information obtained from the D-AHP analysis serves as the reward signal in the DRL algorithm, guiding the optimization of path planning. This ensures that the inspection process prioritizes critical equipment while minimizing the total path length. By employing this method, differences in equipment priorities across various substations can be intuitively compared, validating the applicability and effectiveness of the improved DRL algorithm for multi-objective inspection tasks.

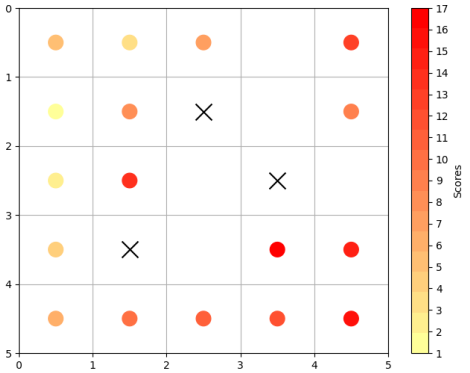

(a)

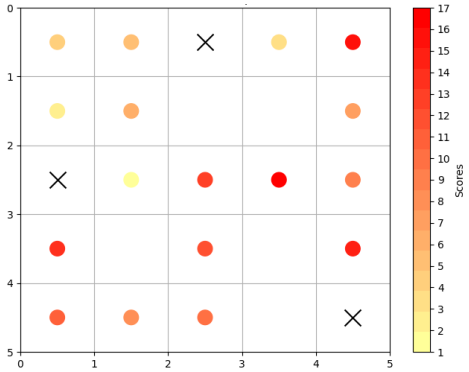

(b)

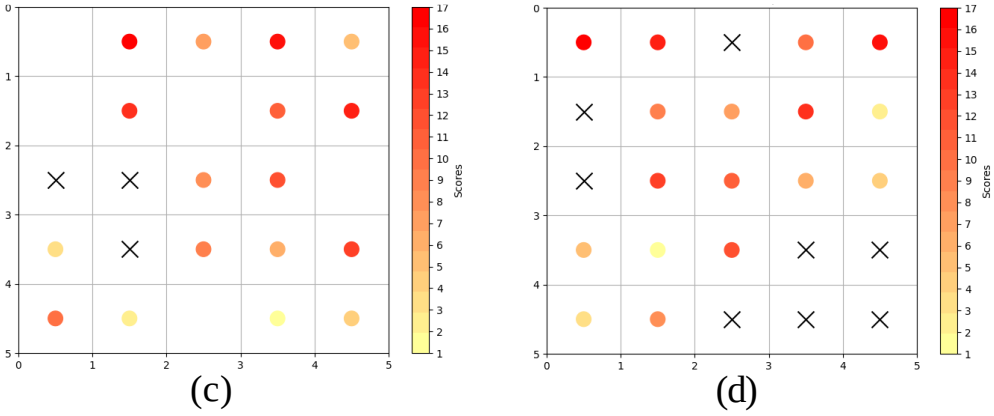

Figure 9. Gridded condition assessment maps of different compartments.

In the path optimization process, this study employs an improved deep reinforcement learning (DRL) algorithm that integrates simulated annealing and pruning techniques. Simulated annealing effectively mitigates the risk of getting trapped in local optima, while pruning reduces the search space by eliminating irrelevant paths and insignificant nodes, thereby accelerating the path search process. The DRL network optimizes the inspection path by learning the relationship between equipment priorities and path costs, thereby ensuring that critical equipment is prioritized during inspection. Specifically, the policy network in the DRL framework selects the optimal action based on the current state, while the value network evaluates the current policy and provides reward signals as feedback to guide the path optimization process.

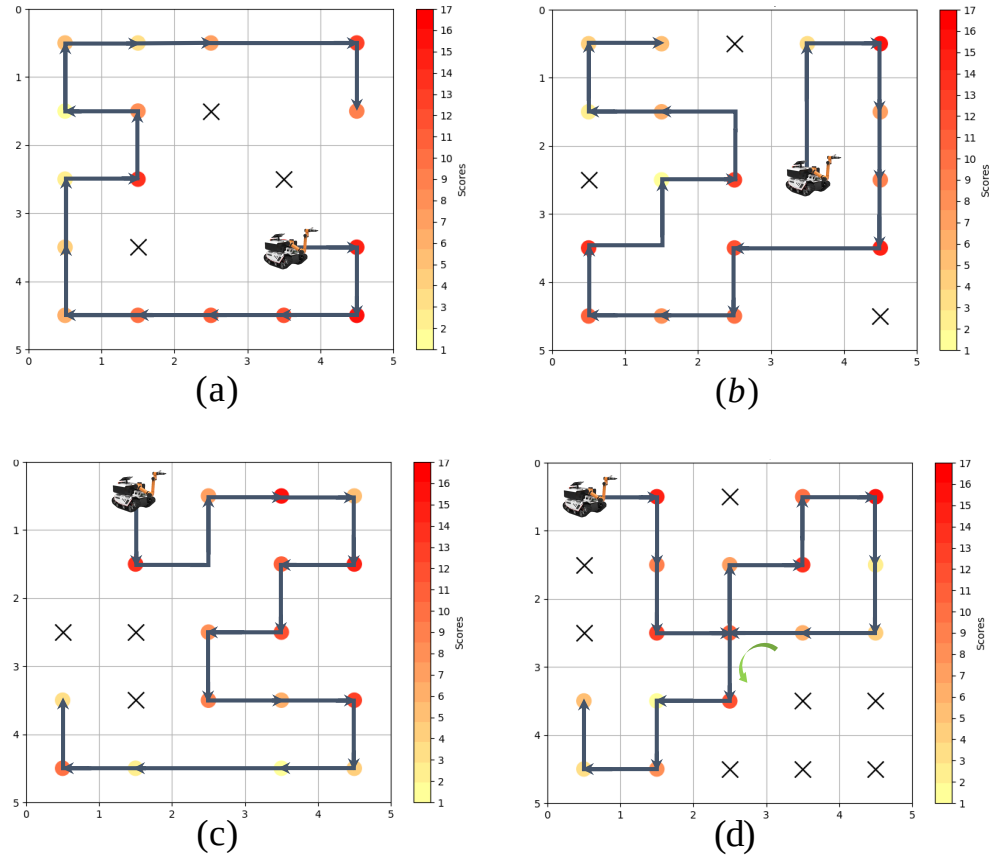

Figure 10. The path planning results obtained by the model proposed in this study.

Figure 10 presents the inspection paths optimized by the proposed improved deep reinforcement learning (DRL) algorithm. The experimental results demonstrate that the algorithm significantly enhances path planning performance by minimizing total path length while prioritizing the inspection of high-priority electrical equipment. Specifically, Blocks (a), (b),

and (c) highlight the algorithm's ability to achieve a balance between path length optimization and the prioritization of critical equipment, ensuring that high-priority inspection tasks are completed efficiently with minimal detours. In Block (d), while a slight increase in path length is observed due to the emphasis on inspecting high-priority equipment, the algorithm maintains its efficacy in achieving an optimal trade-off between path efficiency and priority-based task completion. These results underscore the algorithm's ability to ensure comprehensive inspection coverage while maintaining the operational integrity and safety of the equipment.

Table 8. The repetition rate, coverage rate and number of steps of the planning results.

Block	Algorithms	Repeated coverage (%)	Coverage (%)	Step
Block (a)	Ours	0	100	17
	DQN	0	100	17
	Q-learning	0	100	18
	GA	5.3	100	19
Block (b)	Ours	0	100	20
	DQN	0	100	20
	Q-learning	4.7	100	21
	GA	13.6	100	22
Block (c)	Ours	0	100	18
	DQN	5	100	20
	Q-learning	10	100	20
	GA	10.5	100	19
Block (d)	Ours	5.9	100	17
	DQN	5.9	100	17
	Q-learning	5.9	100	17
	GA	11.1	100	18

Table 8 presents the key performance indicators for path planning results across four distinct substation layouts: Block (a), Block (b), Block (c), and Block (d). The comparison includes the proposed improved deep reinforcement learning (DRL) method, Deep Q-Network (DQN), Q-learning, and the genetic algorithm (GA).

In Blocks (a), (b), and (c), the proposed method demonstrates significant superiority in path length optimization compared to Q-learning and GA. Specifically, in Block (a), the proposed method achieves a path length of 17 steps, whereas Q-learning requires 18 steps and GA requires 19 steps. Similarly, in Blocks (b) and (c), the proposed method achieves path lengths of 20 and 18 steps, respectively, outperforming both Q-learning and GA. Although DQN exhibits competitive results with 17 steps in Block (a) and 20 steps in Block (b), the key distinction lies in redundant coverage. Notably, in Block (c), DQN yields a redundant coverage rate of 5%, whereas the proposed method maintains 0%, highlighting its superior ability to eliminate unnecessary path overlaps.

For equipment coverage, all algorithms achieve 100% across all layouts, ensuring thorough inspection of all electrical equipment, particularly high-priority assets. The primary advantage of the proposed method lies in its ability to minimize path length while maintaining 100% equipment coverage. This is particularly evident in Blocks (a), (b), and (c), where the proposed method consistently outperforms Q-learning and GA in minimizing path length while avoiding unnecessary overlaps. Although DQN also achieves effective results, its slightly higher redundant coverage suggests suboptimal path exploration.

In Block (d), although all algorithms achieve 100% equipment coverage, the redundant coverage rate of the proposed method increases to 5.9%, matching those of DQN and Q-learning. This increase, compared to the other three blocks, arises from prioritizing inspections of high-priority equipment, which may result in slight path overlaps to ensure thorough coverage of these critical assets. Despite this, the proposed method still outperforms GA, which exhibits the highest redundant coverage rate at 11.1%. Regarding path length, the proposed method achieves the shortest path with 17

steps, equivalent to DQN and Q-learning but superior to GA, which requires 18 steps. These results further validate the effectiveness of the proposed method in optimizing path length while balancing inspection completeness and path efficiency, even when prioritizing high-priority equipment.

To further validate the effectiveness and stability of the proposed improved DRL algorithm, we analyzed the training process by monitoring the training loss curve, as illustrated in Figure 11. The curve demonstrates a consistent and smooth convergence trend, with the training loss decreasing from 0.020 to 0.0009 over 30 epochs. This gradual reduction in loss indicates that the algorithm achieves stable learning and reliable optimization capabilities. Specifically, the loss curve shows no significant fluctuations or divergence, suggesting that the model effectively adapts to the training data and converges to an optimal solution.

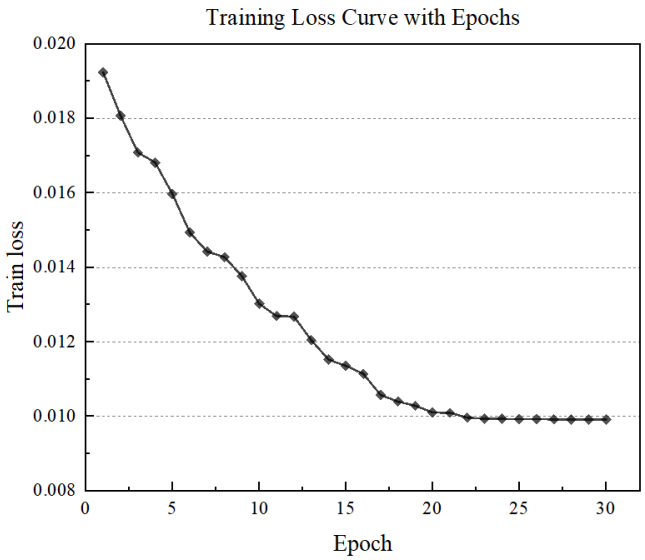

Figure 11. Training loss curve of the proposed DRL algorithm.

In summary, the deep reinforcement learning-based path planning method proposed in this paper not only minimizes path length but also prioritizes the inspection of critical equipment, significantly improving the efficiency and safety of unmanned island substation operations and maintenance. In addition, the DRL-based path planning method proposed in this paper integrates simulated annealing and pruning algorithms to minimize the path length and prioritize the inspection of critical equipment. Specifically, the addition of simulated annealing reduces the risk of local optima, while pruning significantly narrows the search space by eliminating irrelevant paths and nodes. As a result, the total path planning time is reduced to 8m 52.9s, which fully complies with the operational requirements of island substation inspection robots. This efficient planning time, combined with the ability to prioritize high-risk equipment, ensures timely and accurate inspections, thereby enhancing the reliability and safety of island substation operations.

6. Conclusion

This paper proposes an integrated framework for predictive state assessment and path planning in island-based power systems, emphasizing robotic inspections in unmanned environments. The primary contributions include the development of a novel Conv2D-PSE-iTransformer framework, integrating Convolutional Neural Networks (Conv2D), the Parallel Series Embedding (PSE) method, and the iTransformer architecture to provide precise and reliable temperature predictions. Furthermore, a comprehensive health assessment of substation electrical equipment was conducted using the Dynamic Analytic Hierarchy Process (D-AHP). Building on this assessment, we developed a Deep Reinforcement Learning (DRL)-based path planning algorithm that adapts to real-time equipment conditions. The algorithm efficiently prioritizes high-risk areas for inspection while optimizing path lengths to ensure complete coverage. By integrating predictive modeling, dynamic health assessment, and optimized path planning, the proposed method significantly improves the efficiency and accuracy of robotic inspections in complex unmanned environments. This work advances autonomous inspection systems, enhancing the safety, reliability, and operational efficiency of electrical island substations and other high-risk environments.

7. Discussion

While the proposed method demonstrates significant improvements in optimizing inspection time and prioritizing critical equipment, this study has certain limitations that warrant further investigation. Specifically, the performance variations across environments of different complexities, computational cost comparisons with traditional methods, and key metrics such as false detection rate and equipment state prediction accuracy were not extensively analyzed. These limitations stem from the primary focus of this work, which was to introduce a novel framework integrating predictive assessment with inspection path planning, rather than providing

a comprehensive quantitative evaluation.

Future research will address these gaps by evaluating the method's robustness in diverse operational environments, conducting detailed computational cost analyses against traditional approaches, and examining critical performance indicators, including false detection rates and prediction accuracy. These efforts will further validate the method's applicability and provide a more holistic understanding of its performance under varying conditions.

Acknowledge

National Key R&D Program of China (Key Special Project for Marine Environmental Security and Sustainable Development of Coral Reefs 2022-3.1,NO: 2022YFC3102805)

Independent research and development project of Naval Engineering University: Identification of ship cabin equipment based on multispectral images

Reference

1. K.-H. Lee, M.-G. Kim, J. Lee, and P.-S. Lee, "Recent Advances in Ocean Nuclear Power Plants," *Energies,* vol. 8, no. 10, pp. 11470-11492, 2015. https://doi.org/10.3390/en81011470
2. S. Fu, Y. Yu, J. Chen, B. Han, and Z. Wu, "Towards a probabilistic approach for risk analysis of nuclear-powered icebreakers using FMEA and FRAM," *Ocean Engineering,* vol. 260, 2022. https://doi.org/10.1016/j.oceaneng.2022.112041
3. S. E. Hirdaris *et al.*, "Considerations on the potential use of Nuclear Small Modular Reactor (SMR) technology for merchant marine propulsion," *Ocean Engineering,* vol. 79, pp. 101-130, 2014. https://doi.org/10.1016/j.oceaneng.2013.10.015
4. T. Zheng *et al.*, "Nuclear power plant pipeline detection robot based on a new radiation-proof material," *Annals of Nuclear Energy,* vol. 202, 2024. https://doi.org/10.1016/j.anucene.2024.110455
5. I. Tsitsimpelis, C. J. Taylor, B. Lennox, and M. J. Joyce, "A review of ground-based robotic systems for the characterization of nuclear environments," *Progress in Nuclear Energy,* vol. 111, pp. 109-124, 2019. https://doi.org/10.1016/j.pnucene.2018.10.023
6. X. Zhang, C. Sheng, W. Ouyang, and L. Zheng, "Fault diagnosis of marine electric thruster bearing based on fusing multi-sensor deep learning models," *Measurement,* vol. 214, 2023. https://doi.org/10.1016/j.measurement.2023.112727
7. F. Cheng, J. Li, L. Zhou, and G. Lin, "Fragility analysis of nuclear power plant structure under real and spectrum-compatible seismic waves considering soil-structure interaction effect," *Engineering Structures,* vol. 280, 2023. https://doi.org/10.1016/j.engstruct.2023.115684
8. H. Vairagade, S. Kim, H. Son, and F. Zhang, "A nuclear power plant digital twin for developing robot navigation and interaction," *Frontiers in Energy Research,* vol. 12, 2024. https://doi.org/10.3389/fenrg.2024.1356624
9. C. Mineo and Y. Javadi, "Robotic Non-Destructive Testing," *Sensors (Basel),* vol. 22, no. 19, Oct 9 2022. https://doi.org/10.3390/s22197654
10. P. Rea and E. Ottaviano, "Design and development of an Inspection Robotic System for indoor applications," *Robotics and Computer-Integrated Manufacturing,* vol. 49, pp. 143-151, 2018. https://doi.org/10.1016/j.rcim.2017.06.005
11. X. Xu, X. Yan, K. Yang, J. Zhao, C. Sheng, and C. Yuan, "Review of condition monitoring and fault diagnosis for marine power systems," *Transportation Safety and Environment,* vol. 3, no. 2, pp. 85-102, 2021. https://doi.org/10.1093/tse/tdab005
12. A. Mérigaud and J. V. Ringwood, "Condition-based maintenance methods for marine renewable energy," *Renewable and Sustainable Energy Reviews,* vol. 66, pp. 53-78, 2016. https://doi.org/10.1016/j.rser.2016.07.071
13. D. Shanahan, Z. Wang, and A. Montazeri, "Robotics and Artificial Intelligence in the Nuclear Industry: From Teleoperation to Cyber Physical Systems," in *Artificial Intelligence for Robotics and Autonomous Systems Applications*: Springer, 2023, pp. 123-166. https://doi.org/10.1007/978-3-031-28715-2_5
14. J. Cullum, J. Binns, M. Lonsdale, R. Abbassi, and V. Garaniya, "Risk-Based Maintenance Scheduling with application to naval vessels and ships," *Ocean Engineering,* vol. 148, pp. 476-485, 2018. https://doi.org/10.1016/j.oceaneng.2017.11.044
15. J. Zhou, J. Fu, R. Pan, G. Tian, and Y. Li, "Structural design and research of underwater inspection robot for nuclear power plant," presented at the 2022 IEEE Conference on Telecommunications, Optics and Computer Science (TOCS), 2022. https://doi.org/10.1109/TOCS56154.2022.10015995

16. Y. Liu, M. Hajj, and Y. Bao, "Review of robot-based damage assessment for offshore wind turbines," *Renewable and Sustainable Energy Reviews,* vol. 158, 2022. https://doi.org/10.1016/j.rser.2022.112187
17. S.-Y. Park *et al.*, "Digital Twin and Deep Reinforcement Learning-Driven Robotic Automation System for Confined Workspaces: A Nozzle Dam Replacement Case Study in Nuclear Power Plants," *International Journal of Precision Engineering and Manufacturing-Green Technology,* vol. 11, no. 3, pp. 939-962, 2024. https://doi.org/10.1007/s40684-023-00593-6
18. M.-k. Li *et al.*, "Dynamic minimum dose path-searching method for virtual nuclear facilities," *Progress in Nuclear Energy,* vol. 91, pp. 1-8, 2016. https://doi.org/10.1016/j.pnucene.2016.04.001
19. N. M. Thoppil, V. Vasu, and C. S. P. Rao, "Deep Learning Algorithms for Machinery Health Prognostics Using Time-Series Data: A Review," *Journal of Vibration Engineering & Technologies,* vol. 9, no. 6, pp. 1123-1145, 2021. https://doi.org/10.1007/s42417-021-00286-x
20. W. Zhang, Z. Sun, D. Lv, Y. Zuo, H. Wang, and R. Zhang, "A Time Series Prediction-Based Method for Rotating Machinery Detection and Severity Assessment," *Aerospace,* vol. 11, no. 7, 2024. https://doi.org/10.3390/aerospace11070537
21. T. P. Carvalho, F. A. A. M. N. Soares, R. Vita, R. d. P. Francisco, J. P. Basto, and S. G. S. Alcalá, "A systematic literature review of machine learning methods applied to predictive maintenance," *Computers & Industrial Engineering,* vol. 137, 2019. https://doi.org/10.1016/j.cie.2019.106024
22. A. Theissler, J. Pérez-Velázquez, M. Kettelgerdes, and G. Elger, "Predictive maintenance enabled by machine learning: Use cases and challenges in the automotive industry," *Reliability Engineering & System Safety,* vol. 215, 2021. https://doi.org/10.1016/j.ress.2021.107864
23. C. J. Burges, "A tutorial on support vector machines for pattern recognition," *Data mining and knowledge discovery,* vol. 2, no. 2, pp. 121-167, 1998. https://doi.org/10.1023/A:1009715923555
24. S. Liu, Y. Hu, C. Li, H. Lu, and H. Zhang, "Machinery condition prediction based on wavelet and support vector machine," *Journal of Intelligent Manufacturing,* vol. 28, no. 4, pp. 1045-1055, 2015. https://doi.org/10.1007/s10845-015-1045-5
25. X. Li, Q. Ding, and J.-Q. Sun, "Remaining useful life estimation in prognostics using deep convolution neural networks," *Reliability Engineering & System Safety,* vol. 172, pp. 1-11, 2018. https://doi.org/10.1016/j.ress.2017.11.021
26. S. Tapan Kumar and P. Prithwiraj, "Smart Transformer Condition Monitoring and Diagnosis," in *Transformer Ageing: Monitoring and Estimation Techniques*: IEEE, 2017, pp. 403-439. https://doi.org/10.1002/9781119239970.ch9
27. A. Doolgindachbaporn, G. Callender, P. Lewin, E. Simonson, and G. Wilson, "Data Driven Transformer Thermal Model for Condition Monitoring," *IEEE Transactions on Power Delivery,* vol. 37, no. 4, pp. 3133-3141, 2022. https://doi.org/10.1109/TPWRD.2021.3123957
28. A. Bakdi, N. B. Kristensen, and M. Stakkeland, "Multiple Instance Learning With Random Forest for Event Logs Analysis and Predictive Maintenance in Ship Electric Propulsion System," *IEEE Transactions on Industrial Informatics,* vol. 18, no. 11, pp. 7718-7728, 2022. https://doi.org/10.1109/TII.2022.3144177
29. F. Cipollini, L. Oneto, A. Coraddu, A. J. Murphy, and D. Anguita, "Condition-Based Maintenance of Naval Propulsion Systems with supervised Data Analysis," *Ocean Engineering,* vol. 149, pp. 268-278, 2018. https://doi.org/10.1016/j.oceaneng.2017.12.002
30. G. Kabir and R. S. Sumi, "Power substation location selection using fuzzy analytic hierarchy process and PROMETHEE: A case study from Bangladesh," *Energy,* vol. 72, pp. 717-730, 2014. https://doi.org/10.1016/j.energy.2014.05.098
31. P. H. Dos Santos, S. M. Neves, D. O. Sant'Anna, C. H. d. Oliveira, and H. D. Carvalho, "The analytic hierarchy process supporting decision making for sustainable development: An overview of applications," *Journal of Cleaner Production,* vol. 212, pp. 119-138, 2019. https://doi.org/10.1016/j.jclepro.2018.11.270
32. N. Panmala, T. Suwanasri, and C. Suwanasri, "Condition Assessment of Gas Insulated Switchgear Using Health Index and Conditional Factor Method," *Energies,* vol. 15, no. 24, 2022. https://doi.org/10.3390/en15249393
33. H. Tanaka, S. Tsukao, D. Yamashita, T. Niimura, and R. Yokoyama, "Multiple Criteria Assessment of Substation Conditions by Pair-Wise Comparison of Analytic Hierarchy Process," *IEEE Transactions on Power Delivery,* vol. 25, no. 4, pp. 3017-3023, 2010. https://doi.org/10.1109/TPWRD.2010.2048437
34. M. D. P. C. Hernandez and A. Labib, "Selecting a condition monitoring system for enhancing effectiveness of power transformer maintenance," *Journal of Quality in Maintenance Engineering,* vol. 23, no. 4, pp. 400-414, 2017. https://doi.org/10.1108/JQME-07-2015-0027

35. V. González-Prida *et al.*, "Dynamic analytic hierarchy process: AHP method adapted to a changing environment," *Journal of Manufacturing Technology Management,* vol. 25, no. 4, pp. 457-475, 2014. https://doi.org/10.1108/JMTM-03-2013-0030
36. M. Bajaj and A. K. Singh, "An analytic hierarchy process-based novel approach for benchmarking the power quality performance of grid-integrated renewable energy systems," *Electrical Engineering,* vol. 102, no. 3, pp. 1153-1173, 2020. https://doi.org/10.1007/s00202-020-00938-3
37. H. Raharjo, M. Xie, and A. C. Brombacher, "On modeling dynamic priorities in the analytic hierarchy process using compositional data analysis," *European Journal of Operational Research,* vol. 194, no. 3, pp. 834-846, 2009. https://doi.org/10.1016/j.ejor.2008.01.012
38. L. Han, X. Tan, Q. Wu, and X. Deng, "An Improved Algorithm for Complete Coverage Path Planning Based on Biologically Inspired Neural Network," *IEEE Transactions on Cognitive and Developmental Systems,* vol. 15, no. 3, pp. 1605-1617, 2023. https://doi.org/10.1109/TCDS.2023.3237612
39. T. T. Mac, C. Copot, D. T. Tran, and R. De Keyser, "Heuristic approaches in robot path planning: A survey," *Robotics and Autonomous Systems,* vol. 86, pp. 13-28, 2016. https://doi.org/10.1016/j.robot.2016.08.001
40. B. Zhao, C.-d. Wu, X. Zhao, R.-h. Sun, and Y. Jiang, "Research on hybrid navigation algorithm and multi-objective cooperative planning method for electric inspection robot," *Energy Reports,* vol. 9, pp. 805-813, 2023. https://doi.org/10.1016/j.egyr.2023.05.204
41. H. Azpúrua *et al.*, "Towards Semi-autonomous Robotic Inspection and Mapping in Confined Spaces with the EspeleoRobô," *Journal of Intelligent & Robotic Systems,* vol. 101, no. 4, 2021. https://doi.org/10.1007/s10846-021-01321-5
42. Z. Khanam, S. Saha, S. Ehsan, R. Stolkin, and K. McDonald-Maier, "Coverage Path Planning Techniques for Inspection of Disjoint Regions With Precedence Provision," *IEEE Access,* vol. 9, pp. 5412-5427, 2021. https://doi.org/10.1109/ACCESS.2020.3044987
43. J. Clifton and E. Laber, "Q-Learning: Theory and Applications," *Annual Review of Statistics and Its Application,* vol. 7, no. 1, pp. 279-301, 2020. https://doi.org/10.1146/annurev-statistics-031219-041220
44. E. S. Low, P. Ong, and K. C. Cheah, "Solving the optimal path planning of a mobile robot using improved Q-learning," *Robotics and Autonomous Systems,* vol. 115, pp. 143-161, 2019. https://doi.org/10.1016/j.robot.2019.02.013
45. Y. Yu, Y. Liu, J. Wang, N. Noguchi, and Y. He, "Obstacle avoidance method based on double DQN for agricultural robots," *Computers and Electronics in Agriculture,* vol. 204, 2023. https://doi.org/10.1016/j.compag.2022.107546
46. S. R. Barros dos Santos, S. N. Givigi, and C. L. Nascimento, "Autonomous Construction of Multiple Structures Using Learning Automata: Description and Experimental Validation," *IEEE Systems Journal,* vol. 9, no. 4, pp. 1376-1387, 2015. https://doi.org/10.1109/JSYST.2014.2374334
47. Y.-H. Wang, T.-H. S. Li, and C.-J. Lin, "Backward Q-learning: The combination of Sarsa algorithm and Q-learning," *Engineering Applications of Artificial Intelligence,* vol. 26, no. 9, pp. 2184-2193, 2013. https://doi.org/10.1016/j.engappai.2013.06.016
48. A. Fotouhi, M. Ding, and M. Hassan, "Deep Q-Learning for Two-Hop Communications of Drone Base Stations," *Sensors (Basel),* vol. 21, no. 6, Mar 11 2021. https://doi.org/10.3390/s21061960
49. B. Hadi, A. Khosravi, and P. Sarhadi, "Deep reinforcement learning for adaptive path planning and control of an autonomous underwater vehicle," *Applied Ocean Research,* vol. 129, 2022. https://doi.org/10.1016/j.apor.2022.103326
50. A. Krishna Lakshmanan *et al.*, "Complete coverage path planning using reinforcement learning for Tetromino based cleaning and maintenance robot," *Automation in Construction,* vol. 112, 2020. https://doi.org/10.1016/j.autcon.2020.103078
51. J. Ren, X. Huang, and R. N. Huang, "Efficient Deep Reinforcement Learning for Optimal Path Planning," *Electronics,* vol. 11, no. 21, 2022. https://doi.org/10.3390/electronics11213628
52. J. Xu, X. Jiang, S. Liao, D. Ke, Y. Sun, and L. Yao, "Enhanced feature combinational optimization for multivariate time series based dynamic early warning in power systems," *Expert Systems with Applications,* vol. 252, p. 123985, 2024. https://doi.org/10.1016/j.eswa.2024.123985
53. X. Feng and Z. Lyu, "How features benefit: parallel series embedding for multivariate time series forecasting with transformer," in *2022 IEEE 34th International Conference on Tools with Artificial Intelligence (ICTAI)*, 2022: IEEE, pp. 967-975. https://doi.org/10.1109/ICTAI56018.2022.00148
54. A. Krizhevsky, I. Sutskever, and G. E. Hinton, "ImageNet classification with deep convolutional neural networks," *Communications of the ACM,* vol. 60, no. 6, pp. 84-90, 2017. https://doi.org/10.1145/3065386

55. S. Li *et al.*, "Enhancing the locality and breaking the memory bottleneck of transformer on time series forecasting," *Advances in neural information processing systems,* vol. 32, 2019.
56. Y. Liu *et al.*, "itransformer: Inverted transformers are effective for time series forecasting," *arXiv preprint arXiv:2310.06625,* 2023.
57. A. Vaswani, "Attention is all you need," *Advances in Neural Information Processing Systems,* 2017.
58. X. Zhang, E. Gockenbach, V. Wasserberg, and H. Borsi, "Estimation of the Lifetime of the Electrical Components in Distribution Networks," *IEEE Transactions on Power Delivery,* vol. 22, no. 1, pp. 515-522, 2007. https://doi.org/10.1109/TPWRD.2006.876661
59. R. E. Brown and T. M. Taylor, "Modeling the impact of substations on distribution reliability," *IEEE Transactions on Power Systems,* vol. 14, no. 1, pp. 349-354, 1999. https://doi.org/10.1109/59.744554
60. G. Improta, G. Converso, T. Murino, M. Gallo, A. Perrone, and M. Romano, "Analytic Hierarchy Process (AHP) in Dynamic Configuration as a Tool for Health Technology Assessment (HTA): The Case of Biosensing Optoelectronics in Oncology," *International Journal of Information Technology & Decision Making,* vol. 18, no. 05, pp. 1533-1550, 2019. https://doi.org/10.1142/S0219622019500263
61. Y. Wu, W. Song, Z. Cao, J. Zhang, and A. Lim, "Learning improvement heuristics for solving routing problems," *IEEE transactions on neural networks and learning systems,* vol. 33, no. 9, pp. 5057-5069, 2021. https://doi.org/10.1109/TNNLS.2021.3068828
62. International Electrotechnical Commission (IEC). (2005). IEC 60076-7: Power transformers - Part 7: Loading guide. Geneva: IEC